# A Theoretical Study on the Relative Strengths of the Metal-Hydrogen and Metal-Methyl Bonds in Complexes of Middle to Late Transition Metals

**Tom Ziegler,*† Vincenzo Tschinke,† and Axel Becke‡**

*Contribution from the Department of Chemistry, University of Calgary, Calgary, Alberta, Canada, and Department of Chemistry, Queens University, Kingston, Ontario, Canada.*
*Received August 4, 1986*

**Abstract:** Molecular orbital calculations based on density functional theory have been carried out on the homolytic metal-hydrogen and metal-methyl bond energies for MX (M = Cr, Mo, Cu, Ag), $MX^+$ (M = Mn, Tc, Zn, Cd), $XM(CO)_5$ (M = Mn, Tc, Re), and $XM(CO)_4$ (M = Co, Rh, Ir) as well as $XNi(CO)_4^+$ and $XFe(CO)_5^+$ with X = H, $CH_3$. The M-$CH_3$ bonds in the neutral $MCH_3$ and $CH_3M(CO)_n$ molecules are shown to be weaker than the corresponding M-H bonds in MH and $HM(CO)_n$ as a result of exchange repulsions between occupied metal orbitals and the fully occupied $\sigma$-orbital on $CH_3$. For the positively charged species $MCH_3^+$ and $CH_3M(CO)_n^+$ the occupied metal orbitals are contracted in the presence of the positive charge and the exchange repulsions with the fully occupied $\sigma$-orbitals on $CH_3$ as a result reduced to the point where the M-$CH_3$ bond becomes stronger than, or as strong as, the M-H bond. The strength of the M-$CH_3$ bond in $MCH_3^+$ and $CH_3M(CO)_n^+$ is further enhanced as a result of electron charge transfer from the occupied $\pi$-type orbitals on $CH_3$ to unoccupied $d_\pi$ or $p_\pi$ orbitals on M, induced by the positive charge on the metal. The strengths of the M-H and M-$CH_3$ bonds in $XM(CO)_n$ are shown to increase down each of the two triads M = Mn, Tc, Re and M = Co, Rh, Ir as a result of an increase in the $\sigma$-bonding overlaps as well as a stabilizing contribution from relativistic effects for M = Re and Ir. A discussion is finally given on the relation between periodic trends of the homolytic $D(H-M(CO)_n)$ bond energies and the proton affinities of $M(CO)_n^-$. It is, in particular, shown that $Mn(CO)_5^-$ has a larger proton affinity than $Co(CO)_4^-$ as a result of $Co(CO)_4$ having a higher electron affinity than $Mn(CO)_5$.

## I. Introduction

The breaking or formation of metal-hydrogen and metal-alkyl bonds is an integral part of most elementary reaction steps in organometallic chemistry. Considerable efforts have, as a consequence, been directed toward the determination of M-H[1] and M-alkyl[2] bond strengths as a prerequisite for a full characterization of the reaction enthalpies of elementary key steps in organometallic chemistry.

The still scanty data for alkyl[3,4] and hydride[4,5] complexes of middle to late transition metals indicate that the M-H bond is stronger than the M-R bond by some 40-80 kJ $mol^{-1}$ for neutral ligand free MX systems[4] as well as neutral $XML_n$ (X = H, $CH_3$) complexes[4d] with several coligands L. This difference in strength has implications for the relative ease by which ligands can insert into the M-H and M-R bonds[6] as well as the facility[7,8] by which $H_2$ can add oxidatively to a metal center in comparison to H-R and R-R bonds.

We have carried out calculations on M-X (X = H, $CH_3$) bond energies in $XM(CO)_5$ (M = Mn, Tc, Re), $XM(CO)_4$ (M = Co, Rh, Ir), and MX (M = Cr, Mo, Cu, Ag) with middle to late transition metals utilizing density functional theory[9] as well as the program system by Baerends et al.[10] and provide in the first section an analysis of the factors responsible for the difference in strength between the M-H and M-$CH_3$ bonds.

Beauchamp[4a] and Armentrout[4b] and their co-workers have demonstrated that a positive metal center in $MCH_3^+$ is able to stabilize the M-$CH_3$ bond to the extent where it becomes stronger than the corresponding M-H bond in $MH^+$, and we shall, in connection with calculations on $MX^+$ (M = Mn, Tc, Zn, Cd), discuss the origin of this remarkable stabilization in the second section, where it, in addition, will be shown from calculations on $XNi(CO)_4^+$ and $XFe(CO)_5^+$ that a similar stabilization of the M-$CH_3$ bond takes place in positively charged methyl complexes $CH_3ML_n^+$ with several coligands.

The proton affinity of a transition metal fragment $ML_n^-$ is related to the homolytic M-H bond energy of $HML_n$ as well as the electron affinity of $ML_n$. We shall in the third section, as an extension to our calculations on the M-H bond strength in $HM(CO)_n$, present a discussion on the relation between periodic trends in the M-H bond energies of $HM(CO)_n$ and the proton affinities of $M(CO)_n^-$.

## II. Computational Details

The Hartree-Fock-Slater (HFS) or X$\alpha$ method[11] has been used extensively as a model in electron structure calculations on transition-metal complexes. The HFS method is, however, an approximation to the density functional theory of Kohn and Sham[12] in much the same way as *ab initio* Hartree-Fock theory is an approximation to many body theories, including configuration interaction, since both methods completely neglect the correlation between electrons of different spins.[13] Recent advances in density functional theory,[14] which in many ways parallels the development of post-HF methods, have led to remedies for the lack of correlation between electrons of different spins and other short-comings

† University of Calgary.
‡ Queens University.

(1) Pearson, R. G. *Chem. Rev.* **1986**, *85*, 41.
(2) Halpern, J. *Acc. Chem. Res.* **1982**, *15*, 238.
(3) (a) Bruno, J. W.; Marks, T. J.; Mors, L. R. *J. Am. Chem. Soc.* **1983**, *105*, 6824. (b) Georgiadis, R.; Armentrout, P. B. *J. Am. Chem. Soc.* **1986**, *108*, 2119. (c) Aristov, N.; Armentrout, P. B. *J. Am. Chem. Soc.* **1986**, *108*, 1806.
(4) (a) Mandich, M. L.; Halle, L. F.; Beauchamp, J. L. *J. Am. Chem. Soc.* **1984**, *106*, 4403. (b) Armentrout, P. B.; Halle, L. F.; Beauchamp, J. L. *J. Am. Chem. Soc.* **1981**, *103*, 6501. (c) Halle, L. F.; Armentrout, P. B.; Beauchamp, J. L. *Organometallics* **1982**, *1*, 963. (d) Connor, J. A.; Zafarani-Moattar, M. T.; Bickerton, J.; El Saied, N. I.; Suradi, S.; Carson, R.; Al Takhin, G. A.; Skinner, H. A. *Organometallics* **1982**, *1*, 1166.
(5) (a) Squires, R. R. *J. Am. Chem. Soc.* **1985**, *107*, 4385. (b) Sallans, L.; Lane, K. R.; Squires, R.; Freiser, B. S. *J. Am. Chem. Soc.* **1985**, *107*, 4379. (c) Schilling, J. B.; Goddard, W. A., III; Beauchamp, J. L. *J. Am. Chem. Soc.*, in press. (d) Girling, R. B.; Grebenik, P.; Perutz, R. N. *Inorg. Chem.* **1986**, *24*, 31. (e) Ungvary, F. *J. Organomet. Chem.* **1972**, *36*, 363.
(6) Ziegler, T.; Versluis, L.; Tschinke, V. *J. Am. Chem. Soc.*, in press.
(7) Crabtree, R. H. *Chem. Rev.* **1985**, *85*, 245.
(8) Low, J. J.; Goddard, W. A., III *Organometallics* **1986**, *5*, 609.
(9) Becke, A. *J. Chem. Phys.* **1986**, *84*, 4524.
(10) Baerends, E. J.; Ellis, D. E.; Ros, P. *Chem. Phys.* **1973**, *2*, 71.
(11) Slater, J. C. *Adv. Quantum Chem.* **1972**, *6*, 1.
(12) Kohn, W.; Sham, L. J. *Phys. Rev.* **1965**, *140*, A1133.
(13) Ziegler, T.; Rauk, A.; Baerends, E. J. *Theor. Chim. Acta* **1977**, *43*, 261.
(14) (a) Dreizler, R. M.; da Providencia, J, Eds. *Density Functional Methods in Physics*; Plenum: New York, 1985. (b) Avery, J.; Dahl, J. P., Eds. *Local Density Approximations in Quantum Chemistry and Solid State Physics*; Plenum: New York, 1984. (c) Erdahl, R. M.; Smith, V. H., Jr., Eds. *Density Matrices and Density Functionals*; D. Reidel: Dordrecht, in press.

0002-7863/87/1509-1351$01.50/0 

of the HFS method by including two corrections to the HFS-energy expression $E_{HFS}$:

$$E_{BS} = E_{HFS} + E_C + E_X^{NL} \quad (1)$$

The first correction term $E_C$ in eq 1, proposed by Stoll et al.,[15] represents the correlation between electrons of different spins, whereas the second correction term $E_X^{NL}$, due to Becke,[9] represents a nonlocal correction to the HFS-exchange energy $E_X$ of the form

$$E_X^{NL} = \sum_\sigma -\beta \int \frac{[\nabla\rho^\sigma(1)]^2}{[\rho^\sigma(1)]^{4/3}} \left[ 1 + \gamma \frac{[\nabla\rho^\sigma(1)]^2}{[\rho^\sigma(1)]^{8/3}} \right]^{-1} \quad (2)$$

where $\beta$ and $\gamma$ are global parameters[9] and $\rho^\sigma$ with $\sigma = 1$ or $-1$ is the density of electrons with spin up or spin down, respectively. All calculations presented here were based on the LCAO-HFS program system due to Baerends et al.,[10] or its relativistic extension due to Snijders et al.,[16] with only minor modifications to allow for Beck's nonlocal exchange correction as well as the correlation between electrons of different spins in the formulation by Stoll et al., based on Vosko's parametrization[17] from electron gas data. Bond energies were evaluated by the generalized transition-state method[18] or its relativistic extension.[19]

The molecular orbitals were expanded in an uncontracted triple-$\zeta$ STO basis set.[20a,b] The total molecular electron density was fitted in each SCF-iteration by an auxiliary basis[20b] of s, p, d, f, and g STOs centered on the different nuclei in order to represent the Coulomb and exchange potential accurately. Geometrical parameters with the exception of M–H and M–$CH_3$ distances were taken from ref 21.

## III. Initial Consideration

We shall here, for the sake of clarity, specify some of the key concepts used later in the analyses of our numerical results. The concepts are not novel and have, in fact, been dealt with in several recent text books.[22]

The interaction between two orbitals $\Psi_1$ and $\Psi_2$, **1**, separated in energy by $\Delta E = \epsilon_1 - \epsilon_2$ where $\Delta E < 0$ will result in a bonding combination $\Psi_+$ of energy $\epsilon_+ = \epsilon_1 - \Delta E_1$ as well as an antibonding combination $\Phi_-$ or energy $\epsilon_+ = \epsilon_2 + \Delta E_2$.

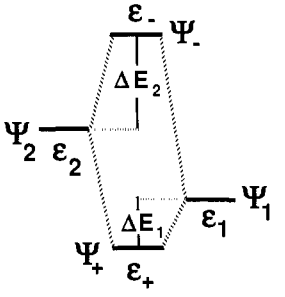


**1**

The orbital $\Psi_-$ will usually be raised more in energy (by $\Delta E_2$) compared to $\Psi_2$ than $\Psi_+$ will be lowered (by $\Delta E_1$) compared to $\Psi_1$, thus

$$\Delta E_2 > \Delta E_1 > 0 \quad (3)$$

The interaction **1** will, in the case where $\Psi_1$ and $\Psi_2$ are both fully occupied, be destabilizing since one pair of electrons after the interaction will be raised more in energy (by $\Delta E_2$) than the other pair will be lowered (by $\Delta E_1$) in energy. Such an interaction is often referred to as a four-electron two-orbital repulsion.[22] The four-electron two-orbital repulsion might be divided up into two interactions **2a** and **2b** each involving a pair of electrons with the same spins. We shall refer to **2a** and **2b** as exchange repulsion interactions.[23]

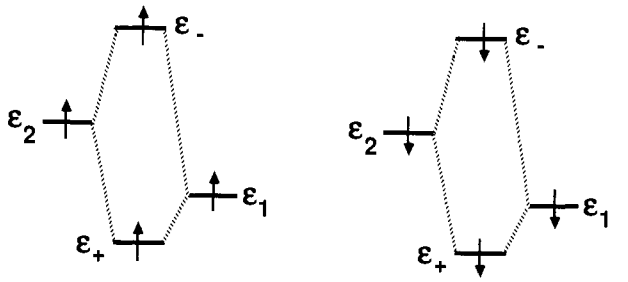


**2 a** **2 b**

A three-electron two-orbital interaction with $\Psi_1$ fully occupied and $\Psi_2$ holding a single electron will result in one exchange repulsion **2** as well as one stabilizing interaction **3a**. The diagram **3a** represents charge polarization[23a,b] if $\Psi_1$ and $\Psi_2$ are on the same fragment and charge transfer if $\Psi_1$ and $\Psi_2$ are on different

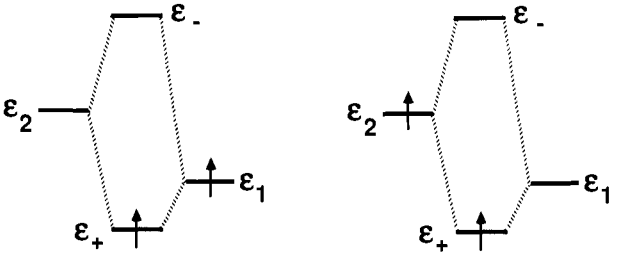


**3 a** **3 b**

fragments. A three-electron two-orbital interaction will in most cases be destabilizing since $\Delta E_2$ often is larger than $2\Delta E_1$. A two-electron two-orbital interaction will, on the other hand, irrespective of the initial configurations $\Psi_1^2$, $\Psi_2^2$, or $\Psi_1^1\Psi_2^1$, be stabilizing since it can be represented by two diagrams of the type **3**. Interactions such as **3a** and **3b** are in the present set of calculations treated quantitatively. It will, however, in connection with the qualitative discussion of our results, be useful to refer to an approximate expression for $\Delta E_1$ given by[22]

$$\Delta E_1 \simeq -\frac{k\langle\Psi_1|\Psi_2\rangle^2}{\epsilon_1 - \epsilon_2} \quad (4)$$

where in eq 4 $k$ is a constant and $\langle\Psi_1|\Psi_2\rangle$ is the overlap between $\Psi_1$ and $\Psi_2$.

## IV. The Orbitals of the Hydrogen Atom and the Methyl Radical

The hydrogen atom and the methyl radical each have a single half-filled orbital available for $\sigma$-bonding with a transition-metal fragment $ML_n$ or a bare transition metal (ion) $M^{n+}$.

For the hydrogen atom $1s_H$ is virtually the only orbital available on H that can participate in the bonding with $ML_n$ or $M^{n+}$. The methyl radical on the other hand has, in addition to the half-filled $2\sigma_{CH_3}$ orbital, three fully occupied bonding orbitals $1\sigma_{CH_3}$, $\pi_{CH_3}$, and $\pi_{CH_3}$, see Figure 1, as well as the corresponding empty an-

(15) Stoll, H.; Golka, E.; Preuss, H. *Theor. Chim. Acta* **1980**, *55*, 29.
(16) Snijders, G. J.; Baerends, E. J.; Ros, P. *Mol. Phys.* **1979**, *38*, 1909.
(17) Vosko, S. H.; Wilk, L.; Nusair, M. *Can. J. Phys.* **1980**, *58*, 1200.
(18) Ziegler, T.; Rauk, A. *Theor. Chim. Acta* **1977**, *46*, 1. The generalized transition state procedure is not only applicable to the HFS method but can be extended to any energy density functional such as $E_{BS}$.
(19) Ziegler, T.; Snijders, G. J.; Baerends, E. J. *J. Chem. Phys.* **1981**, *74*, 1271.
(20) (a) Snijders, G. J.; Baerends, E. J.; Vernooijs, P. *At. Nucl. Data Tables* **1982**, *26*, 483. (b) Vernooijs, P.; Snijders, G. J.; Baerends, E. J. "Slater type basis functions for the whole periodic system", Internal Report; Free University: Amsterdam, The Netherlands, 1981. (c) Krijn, J.; Baerends, E. J. "Fit functions in the HFS-method", Internal Report (in Dutch); Free University: Amsterdam, The Netherlands, 1984.
(21) Ziegler, T. *Organometallics* **1985**, *4*, 675.
(22) Albright, T. A.; Burdett, J. K.; Whangbo, M. H. *Orbital Interactions in Chemistry*; Wiley: New York, 1985; and references therein.
(23) For discussions on the origin of the exchange repulsion see: (a) Fujimoto, H.; Pukui, K. *Adv. Quantum Chem.* **1972**, *6*, 177. (b) Kitaura, K.; Morokuma, K. *Int. J. Quantum Chem.* **1976**, *10*, 325. (c) Whangbo, M. H.; Schlegel, H. B.; Wolfe, S. *J. Am. Chem. Soc.* **1977**, *99*, 1296.

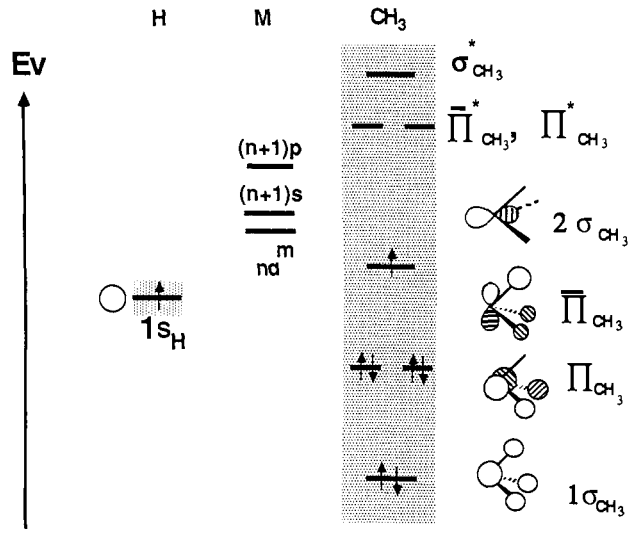


**Figure 1.** Energies for the orbitals of $CH_3$ and H relative to *n*d, $(n + 1)$s, and $(n + 1)$p energy levels of a transition metal M, as well as a schematic representation of the orbitals in $CH_3$.

tibonding orbitals $\sigma^*_{CH_3}$, $\pi^*_{CH_3}$ and $\bar{\pi}^*_{CH_3}$, see Figure 1.

The methyl radical is planar in the free state, **4a**. Complexed methyl, however, has a trigonal pyramidal conformation **4b** with an HCH angle close to 109°. We find from our calculation conformation **4a** to be 25 kJ mol$^{-1}$ more stable than **4b**. The

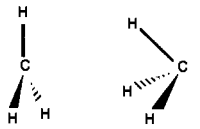

**4a** **4b**

various orbitals of $CH_3$ in conformation **4b** are given schematically in Figure 1.

The primary interaction in $MH^{n+}$ and $MCH_3^{n+}$ involves the two singly occupied ligand orbitals $1s_H$ and $2\sigma_{CH_3}$, respectively, and the at least partly occupied $(n + 1)$s,*n*d$_{z^2}$ orbitals on $M^{n+}$ **5** and **6**, whereas the corresponding key interaction in $HML_n$ and $CH_3ML_n$, for the cases considered here with $ML_n = M(CO)_4^{n+}$ and $M(CO)_5^{n+}$, is between a singly occupied (s,p,d$_{z^2}$)-hybride orbital on $ML_n$ and the half-filled $1s_H$,$2\sigma_{CH_3}$ orbitals, respectively, **7**.

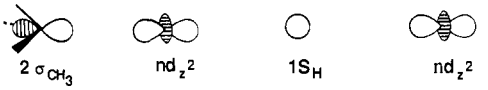


**5a** **5b**

It follows from Figure 1 that $1s_H$ and $2\sigma_{CH_3}$ are of lower energy than the metal $\sigma$-orbitals. However, $2\sigma_{CH_3}$ is above $1s_H$ in energy since $IP_{CH_3}$ = 9.6 eV compared to $IP_H$ = 13.6 eV. Thus, if $\Delta E_1$ is taken as a measure for the strengths of the interactions in **5**–**7** then the demoninator in eq 4, $\epsilon_1 - \epsilon_2$, would make the methyl interactions **5a**, **6a**, and **7a** stronger than the hydrogen interactions **5b**, **6b**, and **7b**. The $1s_H$ orbital on the other hand forms better overlaps with the $\sigma$-metal orbitals than $2\sigma_{CH_3}$. For M = Cr and $ML_n = Co(CO)_4$ we calculate the overlaps **5a**, **6a**, and **7a** as 0.34, 0.14, and 0.32 compared to 0.52, 0.21, and 0.46 for **5b**, **6b**, and **7b**, respectively. Thus the numerator $\langle\Psi_1|\Psi_2\rangle^2$ in eq 4 would strengthen the hydrogen interactions **5b**, **6b**, and **7b** compared to the methyl interactions **5a**, **6a**, and **7a**. A determination of exactly which of the two factors will prevail requires quantitative calculations, and such calculations will be presented in the next sections. It should also be noted that $1s_H$ as well as $2\sigma_{CH_3}$ will have destabilizing three-electron two-orbital interactions with the metal core orbitals, notably *n*s and *n*p$_z$.

It is not sufficient in a comparison between H and $CH_3$ as ligands to restrict the considerations to the relative energies and shapes of $1s_H$ and $2\sigma_{CH_3}$. We must further take into account that $CH_3$, in contrast to H, in addition to a singly occupied $\sigma$-orbital, has several orbitals, both occupied and vacant, that might play a role in the bonding to $M^{n+}$ of $ML_n$.

The occupied orbitals $\pi_{CH_3}$, $\bar{\pi}_{CH_3}$, and in particular $1\sigma_{CH_3}$, Figure 1, can overlap with the *n*s, *n*p core orbitals on the metal, and such overlaps will result in destabilizing exchange repulsion interactions of the type given in **2**. The fully occupied $1\sigma_{CH_3}$ orbital, Figure 1, is further directed in such a way as to form sizable overlaps with $(n + 1)$s, **8a**, as well as *n*d$_{z^2}$, **8b**, and the $\sigma$-hydride orbital on $ML_n$, **8c**. We calculate for $M^{n+}$ = Cr and $ML_n$ = $Co(CO)_4$ the overlaps **8a**, **8b**, and **8c** to be 0.31, 0.16, and 0.26, respectively, which is quite comparable to 0.34, 0.14, and 0.32 calculated for **5a**, **6a**, and **7a**, respectively. The metal orbitals in **8** will, for the systems considered here, hold at least one electron each, and the interactions in **8** will, as a consequence, give rise to destabilizing exchange repulsions, **2**. We shall, in the following sections, show that the exchange repulsions involving $1\sigma_{CH_3}$ play a central role in determining the relative strengths of the M–H and M–$CH_3$ bonds. The two orbitals $\pi_{CH_3}$ and $\bar{\pi}_{CH_3}$, see Figure 1, can overlap


**6a** **6b**

with the *n*d$_\pi$ orbitals on $M^{n+}$, **9a**, or the corresponding $\pi$-type orbitals on $ML_n$, **9b**. The overlaps **9a**, **9b** are far from negligible. In the case of $M^{n+}$ = Cr, **9a** was calculated to be 0.13 with **9b** given by 0.11 for $ML_n$ = $Co(CO)_4$.

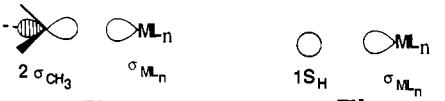


**7a** **7b**

For systems involving early transition metals or f-block elements, where nd$_\pi$ might be vacant, both **9a** and **9b** would represent stabilizing polarization interactions, **3a** and **10**, reminiscent of the hyperconjugation stabilization in organic molecules

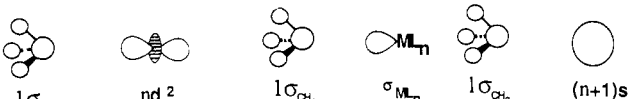


**8a** **8c** **8b**

Among the molecules considered here $CrCH_3$, $MnCH_3^+$, $MoCH_3$, and $TcCH_3^+$ have one electron in each nd$_\pi$ orbital, and **9** will, as a consequence, give rise to one stabilizing polarization interaction, **3a** and **10**, as well as one exchange repulsion **2b**. The other molecules under consideration $ZnCH_3^+$, $CuCH_3$, $CdCH_3^+$, $AgCH_3$, as well as $CH_3M(CO)_4$ and $CH_3M(CO)_5$ have all nd$_\pi$ orbitals fully occupied, and **9** will, as a consequence, in these cases only give rise to exchange repulsions. Charge-transfer stabilizations of the type **10** are, however, possible even for systems where nd$_\pi$ is fully occupied by way of interactions between $\pi_{CH_3}$, $\bar{\pi}_{CH_3}$ and the empty $(n + 1)$p$_\pi$ metal orbitals, **11**. One might have


**9a** **9b**

expected that the virtual orbitals $\sigma^*_{CH_3}$, $\pi^*_{CH_3}$, and $\bar{\pi}^*_{CH_3}$ on $CH_3$ could have given rise to charge-transfer stabilizations of the type

$$M^{\frac{n+}{}}CH_3 \longrightarrow M^{\frac{(n+1)+}{}}CH_3^- \qquad (5)$$

**Table I.** Calculated Bond Energies (kJ mol$^{-1}$) and Bond Distances (Å) for MX and MX$^+$ (X = H, $CH_3$)

| | X = H | | | X = $CH_3$ | | | |
|---|---|---|---|---|---|---|---|
| | $D$(M–X) | $R$(M–X) | | $D$(M–X) | | $R$(M–X) | |
| | calcd | exptl | calcd | exptl | calcd | exptl | calcd |
| $ZnX^+$ | 242 | 238 (–)[a] | 1.54 | 1.52[a] | 288 | 290 (20)[b] | 1.93 |
| CuX | 249 | 276 (8)[a] | 1.47 | 1.46[a] | 238 | | 1.86 |
| $CdX^+$ | 199 | 200 (38)[a] | 1.72 | 1.68[a] | 231 | | 2.15 |
| AgX | 201 | 221 (8)[a] | 1.62 | 1.61[a] | 177 | | 2.06 |
| $MnX^+$ | 193 | 221 (13)[a] | 1.61 | | 234 | 297 (30)[e,f] | 1.95 |
| CrX | 197 | 172 (13)[d] | 1.66 | | 186 | | 2.02 |
| $TcX^+$ | 237 | | 1.68 | | 262 | | 2.11 |
| MoX | 243 | 193 (13)[d] | 1.72 | | 201 | | 2.23 |

[a] Reference 25. [b] Reference 3b. [c] Reference 3c. [d] Reference 5b. [e] Reference 4a. [f] This value is somewhat uncertain owning to difficulty in interpretation of data.

Our calculations indicate, however, that $\sigma^*_{CH_3}$, $\pi^*_{CH_3}$, and $\bar{\pi}^*_{CH_3}$ are too high in energy for (5) to be of any importance, and the high energy of the virtual orbitals on $CH_3$ prevents further $\sigma^*_{CH_3}$, $\pi^*_{CH_3}$, and $\bar{\pi}^*_{CH_3}$ from reducing the exchange repulsion interactions due to **8** and **9** by acting as polarization functions.

## V. Calculations on MX$^+$ (M = Mn, Tc, Zn, Cd; X = H, $CH_3$) and MX (M = Cr, Mo, Cu, Ag; X = H, $CH_3$)

The main objective of our study here has been to compare M–H and M–$CH_3$ bond strengths for metal centers representing middle to late transition elements, leaving methyl and hydride complexes of the electron poor early transition elements for a later investigation.

We shall start out by considering the hydrogen atom and methyl radical bound to a bare transition metal(ion) center $M^{n+}$, where $M^{n+}$ will be represented either by $Mn^+$, Cr, $Tc^+$, and Mo with the $nd^5$ $(n + 1)s^1$ configuration or by $Zn^+$, Cu, $Cd^+$, and Ag with the $nd^{10}$ $(n + 1)s^1$ configuration. Thus, the metal centers will have either a half-filled d-shell or a fully occupied d-shell, and they will further bracket the range of transition elements under investigation here.

**(a) Electronic Ground States for MX$^{n+}$ and Evaluation of the Bond Energy $D$(M–X).** The molecules CrH, $MnH^+$, MoH, and $TcH^+$ had a $^6\Sigma$ ground state corresponding to the $\delta_1^1\delta_2^1\pi_1^1\pi_2^1 1\sigma^2 2\sigma^1$ configuration, whereas $ZnH^+$, CuH, $CdH^+$, and AgH had a $^1\Sigma$ ground state with the $\delta_1^2\delta_2^2\pi_1^2\pi_2^2 1\sigma^2 2\sigma^2$ configuration. Here $\delta_1$, $\delta_2$, $\pi_1$, $\pi_2$ are metal $n$d orbitals of respectively $\delta$ and $\pi$ symmetries and $1\sigma$, $2\sigma$ linear combinations of $1s_H$ and the metal-based $nd_{z^2}$, $(n + 1)$s orbitals.

The molecules $CrCH_3$, $MnCH_3^+$, $MoCH_3$, and $TcCH_3^+$ had under $C_{3v}$ constraints a $^6A_1$ ground state with the $1e_x^1 1e_y^1 2e_x^1 2e_y^1 1a_1^2 2a_1^1$ configuration, whereas $ZnCH_3^+$, $CuCH_3$, $CdCH_3^+$, and $AgCH_3$ had a $^1A_1$ ground state with the $1e_x^2 1e_y^2 2e_x^2 2e_y^2 1a_1^2 2a_1^2$ configuration. The 1e and 2e orbitals were primarily metal base $n$d orbitals of respectively local $\pi$ and $\delta$ axial symmetries, whereas $1a_2$ and $2a_1$ were linear combinations between $2\sigma_{CH_3}$ and the $nd_{z^2}$, $(n + 1)$s metal orbitals.

The $D$(M–H) and $D$(M–$CH_3$) bond energies as well as $R$(M–H) and $R$(M–$CH_3$) bond distances, based on spin-unrestricted calculations, are given in Table I. The $D$(M–H) and $D$(M–$CH_3$) bond energies for MX (X = H, $CH_3$; M = Cr, Mo) and MX$^+$ (X = H, $CH_3$; M = Mn, Tc) were calculated as

$$D(\text{M–X}) = E[\text{X}] + E[nd^5(n + 1)s^1] - E[\text{MX}^{n+}] \quad (6)$$

where $E$[X] is the energy of H or $CH_3$ in conformation **4a** and $E[nd^5(n + 1)s^1]$ is the energy of $M^{n+}$ in the $^6s$ ground state with the $nd^5$ $(n + 1)s^1$ configuration. The bond energies for MX (X = H, $CH_3$; M = Cu, Ag) and MX$^+$ (X = H $CH_3$; M = Zn, Cd) were calculated as

$$D(\text{M–X}) = E[\text{X}] + E[nd^{10}(n + 1)s^1] - E[\text{MX}^{n+}] \quad (7)$$

**(b) Decomposition of $D$(M–H) and $D$(M–$CH_3$).** We shall, in order to explain the trends in Table I, decompose $D$(M–$CH_3$) and $D$(M–H) into a number of terms by considering the formations of $MH^{n+}$ and $MCH_3^{n+}$ in a sequence of steps. We bring in the first step $M^{n+}$ and X = H or X = $CH_3$ in conformation **4b** together to the positions they will take up in MX$^{n+}$, allowing only for the electrostatic interaction $E_{el}$ between $M^{n+}$ and X, while keeping all unpaired electrons on $M^{n+}$ in a $\alpha$-spin state and the odd electron of X = H, $CH_3$ in a $\beta$-spin state. We allow in the second step the occupied orbitals on $M^{n+}$ and X = H, $CH_3$ to overlap and evaluate the sum of the resulting exchange repulsion interactions **2** as $\Delta E_{exrp}$. The sum $\Delta E^\circ = E_{el} + \Delta E_{exrp}$, which we shall refer to as the steric interaction energy, is in exact terms evaluated by constructing the normalized antisymmetrized product function $\Psi_0 = A(\Psi_M\Psi_X)$ from the ground state wave functions of $M^{n+}$ and X and from the corresponding energy $E^\circ$ evaluate $\Delta E^\circ$ as

$$\Delta E^\circ = E[\text{M}] + E[\text{X}] - E^\circ \quad (8)$$

where $E$[M] and $E$[X] are the ground-state energies of $M^{n+}$ and X, respectively. We allow in the third step the density to relax to that of the final molecule $MX^{n+}$, that is, we carry out a full SCF calculation. Thus in the third step the contributions $\Delta E_{TP}$ from all charge-transfer[23a,b] and polarization[23a,b] interactions **3** to the total energy of MX$^{n+}$ are evaluated. Each symmetry representation will contribute to $\Delta E_{TP}$ and we can thus write $\Delta_{TP} = \sum_\Gamma \Delta E_\Gamma$, where $\Gamma$ for $MH^{n+}$ runs over the $\sigma$, $\pi$, and $\delta$ representations and for $MCH_3^{n+}$ over the $A_1$, $A_2$, and E representations. We shall for the sake of uniformity refer to $\Delta E_{A_1}$ as $\Delta E_\sigma$ and to $\Delta E_E$ as $\Delta E_\pi$ since the interactions in $A_1$ and E involve orbitals of local $\sigma$ and $\pi$ symmetries, respectively, in the case of $MCH_3^{n+}$. Adding finally to $D$(M–X) the contributions from relativistic effects $-\Delta E_R$ as well as the energy $\Delta E_{prep} = 25$ kJ mol$^{-1}$ required to deform $CH_3$ from **4a** to **4b** we get the following decomposition

$$D(\text{M–X}) = -E_{el} - \Delta E_{exrp} - \Delta E_\sigma - \Delta E_\pi - \Delta E_R - \Delta E_{prep} \quad (9)$$

A more extensive account of our energy decomposition scheme is given in ref 18 and 24.

**(c) Stabilization of the M–$CH_3$ Bond by a Positive Metal Center.** It follows from Table I that $D$(M–$CH_3$) of $MCH_3^+$ for the same metal M is larger than $D$(M–H) of $MH^+$. This trend contrasts the stability order $D(L_nM\text{–H}) > D(L_nM\text{–}CH_3)$ observed in neutral coordinatively saturated hydride- and methyl–transition-metal complexes as well as the stability order $D$(M–H) > $D$(M–$CH_3$) presented in Table I for the neutral MH and $MCH_3$ molecules.

Mandich, Halle, and Beauchamp[4a] have previously discussed the remarkable strength of the M–$CH_3$ bond in $MCH_3^+$ species and attributed it to a resonant charge stabilization of the metal cation by the methyl ligand **10**, arguing successfully that **10** should be more dominant than the corresponding resonant stabilization

$$\text{M}^+\text{—H} \rightarrow \text{M—H}^+ \quad (10)$$

for $MH^+$, due to the fact that $CH_3$ has a larger polarizability than H.

(24) (a) Ziegler, T.; Rauk, A. *Inorg. Chem.* **1979**, *18*, 1558. (b) Wangbo, M. H.; Schlegel, H. B.; Wolfe, S. *J. Am. Chem. Soc.* **1977**, *99*, 1296.
(25) Huber, K. P.; Herzberg, G. *Molecular Spectra and Molecular Structure*; Van Nostrand Reinhold Co.: New York, 1979; Vol. 4.
(26) (a) Moore, E. J.; Sullivan, J. M.; Nortan, J. R. *J. Am. Chem. Soc.* **1986**, *108*, 2257. (b) Vidal, J. L.; Walker, W. E. *Inorg. Chem.* **1981**, *20*, 249. (c) King, R. B. *J. Am. Chem. Soc.* **1966**, *88*, 5121. (d) Beauchamp, J. L.; Stevens, A. E.; Corderman, R. R. *Pure Appl. Chem.* **1979**, *51*, 967.

**Table II.** Decomposition of Calculated Bond Energies (kJ mol$^{-1}$) $D$(M–X) for $MX^{n+}$ at the Optimized Bond Distances $R$(M–X)

| | $-E_{el}$ | $-\Delta E_{exrp}$ | $\Delta E°$ | $-\Delta E_\sigma$ | $-\Delta E_\pi$ | $-\Delta E_{prep}$ | $-\Delta E_R$ | $D$(M–X)[a] | $R$(M–X) |
|---|---|---|---|---|---|---|---|---|---|
| $MnH^+$ | 137 | −163 | −26 | 221 | | | | 195 | 1.62 |
| CrH | 173 | −199 | −26 | 223 | | | | 197 | 1.66 |
| $MnCH_3^+$ | 304 | −416 | −112 | 311 | 60 | −25 | | 234 | 1.95 |
| $CrCH_3$ | 354 | −500 | −146 | 332 | 25 | −25 | | 186 | 2.02 |
| $ZnCH_3^+$ | 318 | −369 | −51 | 313 | 46 | −25 | 5 | 288 | 1.93 |
| $CuCH_3$ | 424 | −546 | −122 | 363 | 17 | −25 | 5 | 238 | 1.86 |

[a] The bond energy is given as $D(M–X) = \Delta E° - \Delta E_\sigma - \Delta E_\pi - \Delta E_{prep} - \Delta E_R$, where $\Delta E° = -E_{el} - \Delta E_{exrp}$.

**Table III.** Decomposition of $D$(M–H) (kJ mol$^{-1}$) for $MnH^+$ and CrH at $R$(M–H) = 1.66 Å and $D$(M–$CH_3$) for $CrCH_3$ and $MnCH_3^+$ at $R$(M–$CH_3$) = 2.02 Å

| | $-E_{el}$ | $-\Delta E_{exrp}$ | $\Delta E°$ | $-\Delta E_\sigma$ | $-\Delta E_\pi$ | $-\Delta E_{prep}$ | $D$(M–X)[a] |
|---|---|---|---|---|---|---|---|
| $MnH^+$ | 126 | −147 | −21 | 214 | | | 193 |
| CrH | 173 | −199 | −26 | 223 | | | 197 |
| $MnCH_3^+$ | 271 | −323 | −52 | 256 | 50 | −25 | 229 |
| $CrCH_3$ | 354 | −500 | −146 | 332 | 25 | −25 | 186 |

[a] The total bond energy is given as $D(M–X) = \Delta E° - \Delta E_\sigma - \Delta E_\pi - \Delta E_{prep} - \Delta E_R$, where $\Delta E° = -E_{el} - \Delta E_{exrp}$.

We shall here use our energy decomposition scheme to determine the factors responsible for the exceptional strength of the M–$CH_3$ bond in $MCH_3^+$ and provide to this end in Table II the $D$(M–$CH_3$) and $D$(M–H) bond energies of CrH, $CrCH_3$, $MnH^+$, and $MnCH_3^+$ decomposed according to eq 9 at the optimized $R$(M–H) and $R$(M–$CH_3$) bond distances. It might, however, since $MnH^+$ has a shorter bond distance than CrH, Table I, and $MnCH_3^+$ a shorter bond distance than $CrCH_3$, be of interest first to carry out an analysis in which Mn–H and Cr–H on the one hand and Mn–$CH_3$ and Cr–$CH_3$ on the other hand are equidistant. This is done in Table III where $D$(Mn–H) and $D$(Cr–H) both are given the optimized value for CrH and $R$(Mn–$CH_3$) as well as $R$(Cr–$CH_3$) the optimized value for $CrCH_3$.

We note, starting the analysis with CrH and $CrCH_3$, that the overlaps between the occupied orbitals on either H or $CH_3$ and the occupied orbitals on Cr are responsible for the exchange repulsion $\Delta E_{exrp}$ as well as the electrostatic interaction $E_{el}$ (Table III). Without such overlaps both $\Delta E_{exrp}$ and $E_{el}$, and as a consequence $\Delta E°$, would be zero. The methyl radical has, in contrast to H, several occupied orbitals overlapping with occupied orbitals on Cr, and $\Delta E_{exrp}$ for $CrCH_3$ is as a consequence larger than $\Delta E_{exrp}$ for CrH (Table III), with the major part of the difference being made up by the exchange repulsion interactions **8a** and **8b** due to the occupied $1\sigma_{CH_3}$ orbital. The overlaps between occupied orbitals on different fragments have, however, also a stabilizing effect, in that electron density from one fragment (A) will penetrate the shielding of the nuclei on fragment B by the electron density on B, resulting[24] in net stabilizing electron–nucleus attractions. This penetration is, since $CH_3$ as already mentioned in contrast to H has several occupied orbitals, more important for $CrCH_3$ than for CrH. Thus, $-E_{el}$ is larger for $CrCH_3$ than for CrH (Table III). When $-E_{el}$ and $-\Delta E_{exrp}$ are combined into the steric interaction energy $\Delta E° = -E_{el} - \Delta E_{exrp}$ one finds (Table III) that $\Delta E°$ is more destabilizing (negative) for $CrCH_3$ than for CrH.

We note, in turning next to the stabilizing terms $-\Delta E_\sigma$ and $-\Delta E_\pi$ of eq 9, that $-\Delta E_\sigma$ arises from the interactions **5** and **6** and that the relative magnitude of $-\Delta E_\sigma$ in $CrCH_3$ and CrH, as already mentioned, is adversely dependent on the denominator and numerator of eq 4. Our quantitative calculations indicate the $-\Delta E_\sigma$ is larger in $CrCH_3$ than in CrH (Table III). Further, $CrCH_3$, with the occupied $\pi_{CH_3}$ orbitals on $CH_3$ (Figure 1), has in contrast to CrH a modest contribution to $-\Delta E_\pi$ from the charge-transfer interaction **9a**. In summary the sum $-\Delta E_\sigma - \Delta E_\pi$ is seen to be more stabilizing for $CrCH_3$ than for CrH whereas the steric interaction energy $\Delta E°$ is more destabilizing for $CrCH_3$ than for CrH, with the result that $D$(Cr–$CH_3$) of $CrCH_3$, when all terms in eq 9 are combined (including $-\Delta_{prep}$), is marginally smaller than $D$(Cr–H) of CrH (Table III). It should be mentioned, though, that $D$(Cr–$CH_3$) without the contribution from $-\Delta E_{prep}$, representing the energy required to deform $CH_3$ from conformation **4a** to **4b**, would have been marginally larger than $D$(Cr–H).

We are now after the detailed decomposition analysis of $D$(Cr–H) and $D$(Cr–$CH_3$) in a position to account for the factors responsible for the remarkable stability of the Mn–$CH_3$ bond in $MnCH_3^+$. What according to our analysis basically sets $MnCH_3^+$ apart from the isoelectronic $CrCH_3$ molecule is the smaller size of the overlaps between orbitals on $Mn^+$ and orbitals on $CH_3$ in comparison with the corresponding overlaps between orbitals on chromium with the orbitals on $CH_3$, as a consequence of 3d and 4s on the positive $Mn^+$ ion being more contracted than 3d and 4s on the neutral chromium atom. One implication from the difference in the size of the overlaps is that $\Delta E_{exrp}$ and $-E_{el}$, due to the overlaps between occupied orbitals on the metal with occupied orbitals on $CH_3$, are smaller for $MnCH_3^+$ than for $CrCH_3$ (Table III), with the balance $\Delta E°$ being less destabilizing for $MnCH_3^+$ than for $CrCH_3$, primarily as a result of a sizable reduction in the exchange repulsion interaction **8** involving $1\sigma_{CH_3}$ in the case of $MnCH_3^+$.

Any variation in the size of the overlaps between metal orbitals and methyl orbitals is, however, bound to influence the bonding interactions **5a**, **6d**, and **9a** as well as $\Delta E_{exrp}$ and $-E_{el}$, and we see in fact that $-\Delta E_\sigma$ due to **5a** and **6a** is smaller for $MnCH_3^+$ than for $CrCH_3$ (Table III). The positive charge on $Mn^+$ is, to some degree, able to compensate for the smaller bonding overlaps in $MnCH_3^+$ by stabilizing metal to methyl charge transfer (**10**). The charge-transfer stabilization is important for **5a** and **6a**, without it $-\Delta E_\sigma$ would have been even smaller for $MnCH_3^+$, and crucial for **9a** in that $-\Delta E_\pi$ is larger for $MnCH_3^+$ than for $CrCH_3$. When all terms in eq 9 are added up the Mn–$CH_3$ bond in $MnCH_3^+$ is seen to be more stable than the Cr–$CH_3$ bond in $CrCH_3$ by 43 kJ mol$^{-1}$ (Table III).

We have seen how a positive metal center can stabilize a M–$CH_3$ bond by reducing the exchange-repulsion interactions (**8**) as well as enhancing the methyl to metal charge transfer (**9a**) from $\pi_{CH_3}$ to the $nd_\pi$ and $(n+1)p_\pi$ orbitals on the metal. A positive metal center does apparently not have a similar ability to stabilize the M–H bond in $MH^+$ judging from Table III where we in fact calculate the Mn–H bond in $MnH^+$ to be slightly weaker than the Cr–H bond of CrH. This is perhaps not too surprising in view of our analysis of the M–$CH_3$ bond. Thus, the reduction in $\Delta E_{exrp}$ in going from CrH to $MnH^+$, as a result of the contraction of 3d and 4s on $Mn^+$, is, since H lacks fully occupied orbitals such as $1\sigma_{CH_3}$ involved in exchange repulsion, modest and largely balanced by a corresponding reduction in $-E_{el}$. The hydrogen atom lacks further occupied $\pi$-type orbitals, and the positive metal center is as a consequence unable to enhance the M–H bond through ligand-to-metal charge-transfer interactions similar to **9** in the case of $MnCH_3^+$.

We have up to this point considered Mn–H and Cr–H as equidistant at the $R$(Cr–H) bond distance optimized for CrH (Table III) and Cr–$CH_3$ and Mn–$CH_3$ as equidistant at the $R$(Cr–$CH_3$) bond distance optimized for $CrCH_3$, in order to keep as many factors as possible equal in the analysis. The manganese

molecules are, however, calculated to have somewhat shorter bonds than the corresponding chromium systems (Table I). Allowing for this differential by shortening the Mn–X bonds will increase the individual contributions $-E_{el}$, $\Delta E_{exrp}$, $-\Delta E_\sigma$, and $-\Delta E_\pi$ to $D$(Mn–X), as the metal–ligand overlap becomes larger, without changing $D$(Mn–X) by more than a few kJ mol$^{-1}$ (Table III). At their respective equilibrium distances $MnCH_3^+$ is still seen to have a less destabilizing steric interaction energy and a larger contribution from $-\Delta E_\pi$ than $CrCH_3$.

The explanation given here for the remarkable stability of the M–$CH_3$ bond in the positively charged $MnCH_3^+$ molecule of the ($MnH^+$, CrH, $MnCH_3^+$, $CrCH_3$) series applies as well to $TcCH_3^+$, $ZnCH_3^+$, and $CdCH_3^+$ of the respective series ($TcH^+$, MoH, $TcCH_3^+$, $MoCH_3$), ($ZnH^+$, CuH, $ZnCH_3^+$, $CuCH_3$), and ($CdH^+$, AgH, $CdCH_3^+$, $AgCH_3$). Thus, it is evident from Table II, where we present a decomposition of $D$(Cu–$CH_3$) and $D$($Zn^+$–$CH_3$) at the respective equilibrium distances of $CuCH_3$ and $ZnCH_3^+$, that the steric interaction energy $\Delta E°$ is less destabilizing and the contribution from $-\Delta E_\pi$ more stabilizing for $ZnCH_3^+$ compared to $CuCH_3$. The charge transfer from $\pi_{CH_3}$, responsible for $-\Delta E_\pi$, is in $ZnCH_3^+$ and $CuCH_3$ to the $(n+1)p_\pi$ metal orbital, **11**, since $nd_\pi$ is fully occupied in bond Cu and $Zn^+$.

It can be seen from Table I that each of the members in the 4d-series ($TcH^+$, MoH, $TcCH_3^+$, and $MoCH_3$) has a stronger M–X bond than the homologue in the 3d-series ($MnH^+$, CrH, $MnCH_3^+$, and $CrCH_3$). The increase in bond strength down a triad can be attributed to a corresponding increase in the bonding overlaps **6a** and **6b** between either $2\sigma_{CH_3}$ or $1s_H$ and $nd_\sigma$ on the metal. Thus, $\langle 1s_H|nd_\sigma\rangle$ is calculated to be 0.15 and 0.22 for $MnH^+$ and $TcH^+$, respectively. For the series ($ZnH^+$, CuH, $ZnCH_3^+$, and $CuCH_3$) and ($CdH^+$, AgH, $CdCH_3^+$, and $AgCH_3$) one observes (Table I) on the other hand a decrease in the M–X bond strength down a triad. The overlaps **6a** and **6b** are for the group 11 and group 12 molecules destabilizing as $nd_\sigma$ of M = $Zn^+$, Cu, $Cd^+$, and Ag are fully occupied, and an increase in either $\langle 1s_H|nd_\sigma\rangle$ or $\langle 2\sigma_{CH_3}|nd_\sigma\rangle$ down a triad will as a consequence destabilize the M–X bond.

It should be mentioned here that the strength of the M–X bond will increase again as we proceed from the MX molecules of Ag and $Cd^+$ to their 5d homologues of Au and $Hg^+$ due to the influence of relativistic effects. This point has been dealt with in a previous study[19] and will not be discussed further here.

The calculated $D$(M–X) and $R$(M–X) values in Table I are in good to fair agreement with the few available experimental bond energies and bond distances. The uncertainties in the experimental bond energies for $MnH^+$ and $MnCH_3^+$ might be larger than indicated in Table I due to difficulties with the interpretation of the experimental data.[4a] The molecules in Table I all had metal centers with half-filled or completely filled d-shells. Schilling, Goddard, and Beauchamp[5c] have carried out calculations on the complete series of 3d $MH^+$ hydrides with M = Ca, Sc, Ti, V, Mn, Fe, Co, Ni, Cu, and Zn using the GVB–DCCI method.

## VI. Relative Strength of the M–H and M–$CH_3$ Bonds in Saturated Transition-Metal Complexes

The dearth[1] of reliable experimental data on bond dissociation energies is felt throughout the field of organometallic chemistry and is in particular notable with respect to metal–hydrogen and metal–alkyl bond energies in coordinatively saturated transition-metal complexes of group 6 to group 12 elements. Often somewhat qualitative estimates point to the M–$CH_3$ bond as being weaker than the corresponding M–H bond by some 40–80 kJ mol$^{-1}$, and Connor et al.[4d] find in their accurate calorimetric study on $HMn(CO)_5$ and $CH_3Mn(CO)_5$ a difference of 60 kJ mol$^{-1}$.

The preconceived stability order $D(L_nM–H) > D(L_nM–CH_3)$ is consistent with data on organometallic reactions in which M–H and M–$CH_3$ bonds are formed or broken. Thus, CO will readily insert into a M–$CH_3$ bond whereas the corresponding insertions into M–H bonds are virtually unknown,[6] and methyl has likewise a larger migratory aptitude toward most other ligands than hydride. The $H_2$ molecule is further known to add oxidatively and exothermicly to several metal fragments where the corresponding oxidative additions of the H–R and R–R bonds are unknown and probably endothermic as a consequence of the weak M–R bond.[7]

**Table IV.** Calculated Bond Energies (kJ mol$^{-1}$) and Bond Distances (Å) for $XM(CO)_4^+$ and $XM(CO)_5^+$ (X = H, $CH_3$)

| | X = H | | X = $CH_3$ | |
|---|---|---|---|---|
| | $D$(M–X) | $R$(M–X) | $D$(M–X) | $R$(M–X) |
| $XMn(CO)_5$ | 225 | 1.58 | 153 | 2.16 |
| $XTc(CO)_5$ | 252 | 1.63 | 1.78 | 2.26 |
| $XRe(CO)_5$ | 282 (247)[a] | 1.62 | 200 (185)[a] | 2.27 |
| $XCo(CO)_4$ | 230 | 1.55 | 160 | 2.11 |
| $XRh(CO)_4$ | 255 | 1.62 | 190 | 2.23 |
| $XIr(CO)_4$ | 286 (251)[a] | 1.60 | 212 (187)[a] | 2.24 |
| $XFe(CO)_5^+$ | 251 | 1.56 | 239 | 2.12 |
| $XNi(CO)_4^+$ | 258 | 1.51 | 251 | 2.08 |

[a] Nonrelativistic results.

We have calculated the $D(L_nM–H)$ and $D(L_nM–CH_3)$ bond energies for the quintessential methyl and hydride complexes $XMn(CO)_5$ (**12**) and $XCo(CO)_4$ (**13**) as well as their 4d and 5d homologues in order to delineate variations in $D(L_nM–H)$ and $D(L_nM–CH_3)$ along a period and down a triad, and we present the results in Table IV. We calculate for a given $M(CO)_n$ fragment $D$(H–$M(CO)_n$) to be some 70–80 kJ mol$^{-1}$ larger than $D$($CH_3$–$M(CO)_n$) (Table IV). This difference can be analyzed further by decomposing $D$(X–$M(CO)_n$) as

$$D(X–M(CO)_n) = -E_{el} - \Delta E_{exrp} - \Delta E_\sigma - \Delta E_\pi - \Delta E_R - \Delta E_{prep} \quad (11)$$

where $-\Delta E_\sigma$ represents the contribution from the bonding interactions **7a** or **7b** and $-\Delta E_\pi$ represents the contribution from the charge-transfer interaction **11**. The remaining terms in eq 11 have the same meaning as in eq 9. We have in the evaluation of $D$(X–$M(CO)_n$) assumed that the $M(CO)_4$ and $M(CO)_5$ radicals have the same structures as the $M(CO)_4$ and $M(CO)_5$ frameworks in **12** and **13**, respectively, and $\Delta E_{prep}$ corresponds as a consequence only to the deformation of $CH_3$ from **4a** and **4b**. The relaxation energies of the $M(CO)_4$ and $M(CO)_5$ frameworks, which we have assumed to be small here, would to the extent that they are not negligible reduce the bonding energies in Table IV without changing the calculated differences between $D$($CH_3$–$M(CO)_n$) and $D$(H–$M(CO)_n$).

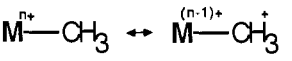


**10**

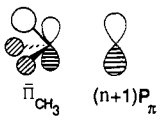


**11**

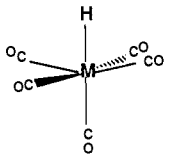


**12**

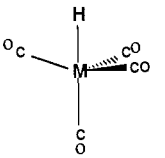


**13**

A decomposition of $D$(X–$Mn(CO)_5$) and $D$(X–$Co(CO)_4$) (X = H, $CH_3$) is presented in Table V. We find as for the neutral ligand free $MCH_3$ and MH molecules that $CH_3M(CO)_n$ has a stronger $\sigma$-bonding interaction **7a** than $HM(CO)_n$ (**7b**), whereas the steric interaction energy $\Delta E°$ is more destabilizing in $CH_3M(CO)_n$ than in $HM(CO)_5$ primarily as a result of the exchange repulsion interaction **8c** involving $1\sigma_{CH_3}$. Combined, the steric interaction energy $\Delta E°$ prevails and we find the stability order $D$(H–$M(CO)_n$) > $D$($CH_3$–$M(CO)_n$) in spite of a modest contribution from $-\Delta E_\pi$ in the case of $CH_3M(CO)_n$.

If a positive metal center is able to stabilize the M–$CH_3$ bond in the ligand-free $MCH_3^+$ molecules then one might expect a similar stabilization from a positive $M(CO)_n^+$ fragment. We have in order to see if in fact such a stabilization takes place calculated $D$(M–H) and $D$(M–$CH_3$) for $CH_3Fe(CO)_5^+$, $HFe(CO)_5^+$, $HNi(CO)_4^+$, and $CH_3Ni(CO)_4^+$ isoelectronic with the neutral $HMn(CO)_5$, $CH_3Mn(CO)_5$, $HCo(CO)_4$, and $CH_3Co(CO)_4$ molecules, respectively (Table IV). It is clear that $D$(M–H), and

**Table V.** Decomposition of Calculated Bond Energies (kJ mol$^{-1}$) $D$(M–X) for $XMn(CO)_5$ and $XCo(CO)_4$ (X = H, $CH_3$) as well as $CH_3Ni(CO)_4^+$ at the Optimized Bond Distances $R$(M–X) (Å)

| | $-E_{el}$ | $-\Delta E_{exrp}$ | $\Delta E°$ | $-\Delta E_\sigma$ | $-\Delta E_\pi$ | $-\Delta E_{prep}$ | $D$(M–X)[a] | $R$(M–X) |
|---|---|---|---|---|---|---|---|---|
| $HMn(CO)_5$ | 258 | −368 | −110 | 335 | | | 225 | 1.58 |
| $CH_3Mn(CO)_5$ | 343 | −545 | −202 | 360 | 20 | −25 | 153 | 2.16 |
| $HCo(CO)_4$ | 258 | −369 | −111 | 341 | | | 230 | 1.55 |
| $CH_3Co(CO)_4$ | 303 | −513 | −210 | 366 | 29 | −25 | 160 | 2.11 |
| $CH_3Ni(CO)_4^+$ | 289 | −440 | −151 | 361 | 66 | −25 | 251 | 2.08 |

[a] The total bonding energy $D$(M–X) is given as $D(M-X) = -E_{el} - \Delta E° - \Delta E_\sigma - \Delta E_\pi - \Delta E_{prep}$, where $\Delta E° = -E_{el} - \Delta E_{exrp}$.

in particular $D(M-CH_3)$, for the positively charged molecules are larger than the corresponding values for the isoelectronic neutral molecules. A decomposition analysis of $D(M-CH_3)$ for $CH_3Ni(CO)_4^+$ reveals further (Table V) that $D(M-CH_3)$ of $CH_3Ni(CO)_4^+$ is enhanced compared to $D(M-CH_3)$ of $CH_3Co(CO)_4$ by a reduction in $\Delta E_{exrp}$ as well as an increase in $-\Delta E_\pi$, representing the charge transfer stabilization interaction **11**. Thus, the factors responsible for the stabilization of the $M-CH_3$ bond by a positive metal center are at work in the stabilization of the $M-CH_3$ bond by a positively charged $M(CO)_n^+$ fragment as well. The findings here would imply that the oxidative addition of C–H or R–R bonds to a positively charged metal fragment should be more facile then the addition to the corresponding isoelectronic neutral fragment.

Considerations up to this point have been given to neutral or positively charged alkyl and hydride carbonyl complexes of 3d transition elements. Proceeding now from $XMn(CO)_5$ and $XCo(CO)_4$ to their 4d and 5d homologues we find (Table IV), in line with experimental data,[1,7] that there is an increase in the M–X bond energies as we descend either of the two triads M = Mn, Tc, Re or Co, Rh, Ir, with a substantial jump in $D$(M–X) between the 3d and 4d homologues and a more modest jump in $D$(M–X) between the 4d and 5d homologues. Those trends correlate with an increase in the bonding overlaps between either $1s_H$ or $2\sigma_{CH_3}$ and the (p,d)-hybride $\sigma_{ML_n}$ on the metal center, **7c**. Thus, we calculate $\langle 1s_H|\sigma_{ML_n}\rangle$ to be 0.41, 0.45, and 0.46 for $HCo(CO)_4$, $HRh(CO)_4$, and $HIr(CO)_4$, respectively. The M–X bond strength for the 5d congeners $XRe(CO)_5$ and $XIr(CO)_4$ is further enhanced by a contribution, $-\Delta E_R$, due to relativistic effects, and it can be seen from Table IV that such effects largely are responsible for the M–X bonds being stronger in the 5d complexes $XRe(CO)_5$ and $XIr(CO)_4$ compared to the corresponding 4d complexes $XTc(CO)_5$ and $XRh(CO)_4$.

The homolytic $D(H-M(CO)_5)$ and $D(H-M(CO)_4)$ bond energies calculated here are in good agreement with the values $D(H-M(CO)_5)$ = 213 kJ mol$^{-1}$ and $D(CH_3-M(CO)_5)$ = 153 kJ mol$^{-1}$, respectively, obtained experimentally by Connor et al.[4d] Ungvary[5e] has further measured $D(H-Co(CO)_4)$ as 238 kJ mol$^{-1}$ in fair agreement with our theoretical value of 230 kJ mol$^{-1}$. There are some uncertainties associated with the experimental values for the bond energies of $HMn(CO)_5$ and $HCo(CO)_4$ due to the assumptions[29] made about the strengths of the metal–metal bonds in $Mn_2(CO)_{10}$ and $Co_2(CO)_8$, respectively. The experimental data for $HMn(CO)_5$ and $HCo(CO)_4$ presented here are, however, in line with the general trend in Table V, according to which $D(X-M(CO)_4) > D(X-M(CO)_5)$ for metals within the same transition series. We shall comment on this point further in the next section in connection with a discussion on the relation between periodic trends in $D(H-N(CO)_n)$ and the proton affinities of $M(CO)_n^-$.

## VII. The Relation between Periodic Trends in the Proton Affinity of $M(CO)_n^-$ and the Homolytic M–H Bond Energy of $MH(CO)_n$

We have in the previous sections calculated the bond energy $D$(M–H) corresponding to the homolytic dissociation

$$H-M(CO)_n \rightarrow H + M(CO)_n \qquad (12)$$

for several carbonyl hydrides.

Somewhat related to the process in eq 12 is the protonic and heterolytic dissociation

$$H-M(CO)_n \rightarrow H^+ + M(CO)_n^- \qquad (13)$$

**Table VI.** Calculated Electron Affinities $A[M(CO)_n]$ (kJ mol$^{-1}$) and Proton Affinities $Pa[M(CO)_n^-]$ (kJ mol$^{-1}$)

| | $D(H-M(CO)_n)$[b] | $A[M(CO)_n]$ | $PA[M(CO)_n^-]$[a] |
|---|---|---|---|
| $HMn(CO)_5$ | 225 | 285 | 1253 |
| $HTc(CO)_5$ | 252 | 250 | 1315 |
| $HRe(CO)_5$ | 282 | 250 | 1345 |
| $HCo(CO)_4$ | 230 | 324 | 1219 |
| $HRh(CO)_4$ | 255 | 319 | 1249 |
| $HIr(CO)_4$ | 286 | 311 | 1288 |
| $HCo(CO)_3(PH_3)$ | 219 | 266 | 1266 |

[a] The proton affinity was calculated as $PA[M(CO)_n] = D(H-M(CO)_n) + 1313 - A[(M(CO)_n]$ according to eq 14. [b] $D(H-M(CO)_n)$ is the homolytic bond dissociation energy from Table V.

for which the corresponding $H-M(CO)_n$ bond energy is given by the proton affinity of $M(CO)_n^-$. The proton affinity $PA[M(CO)_n^-]$ of $M(CO)_n^-$ can be expressed in terms of $D(H-M(CO)_n)$ as well as the ionization potential $IP_H$ for the hydrogen atom and the electron affinity $A[M(CO)_n]$ of the $M(CO)_n$ radical as

$$PA[M(CO)_n^-] = IP_H + D(H-M(CO)_n) - A[M(CO)_n] \qquad (14)$$

The proton affinity of a metal fragment $ML_n^-$ is an interesting property in its own right as well as an important measure for the nucleophilicity of $ML_n^-$, and there has as a consequence been several experimental[7,26] as well as a few theoretical[27] attempts to establish a common proton affinity scale for a broad scope of $ML_n^-$ fragments. The PA scale established to date[26a] exhibits several interesting period trends. It is, however, not clear whether those trends are determined by variations in the homolytic H–M bond energies or by changes in the electron affinities of $ML_n^-$, eq 14.

We present, in order to shed some light on this point in Table VI, theoretical electron affinities for $M(CO)_5$ (M = Mn, Tc, Re) and $M(CO)_4$ (M = Co, Rh, Ir), along with calculated homolytic $D(H-M(CO)_n)$ bond energies for $HM(CO)_5$ (M = Mn, Tc, Re) and $HM(CO)_4$ (M = Co, Rh, Ir) as well as proton affinities $PA[M(CO)_n^-]$ for $M(CO)_5^-$ (M = Mn, Tc, Re) and $M(CO)_4^-$ (M = Co, Rh, Ir), calculated from eq 14 with $IP_H$ taken as 1313 kJ mol$^{-1}$.

The proton affinities $PA[M(CO)_n^-]$ are, in agreement with experiment, calculated to increase on descending either of the two triads M = Mn, Tc, Re and M = Co, Rh, Ir as a result both of an increase in $D(H-M(CO)_n)$ and a decrease in $A[M(CO)_n^-]$, where the decrease in $A[M(CO)_n^-]$ can be understood by observing that the (p,d) metal hybride on $M(CO)_n$,[27b] accepting the extra electron, is more antibonding with respect to the $\sigma_{CO}$ ligand orbitals for the 4d and 5d member of the series than the 3d member.[27b] The 4d and 5d members of the two series are as a consequence less able to stabilize the $M(CO)_n^-$ anion. We expect in most cases the proton affinity for $ML_n^-$ to increase down a triad in a homologous series.

We have, as discussed in the previous section, calculated the homolytic bond energy $D$(H–M) for $HCo(CO)_4$ to be slightly larger than $D$(M–H) of $HMn(CO)_5$. One might thus have expected the proton affinity of $Mn(CO)_5^-$ to be slightly larger than the proton affinity of $Co(CO)_4^-$, provided that $D$(M–H) is the

(27) (a) Bursten, B. E.; Gatter, M. G. *J. Am. Chem. Soc.* **1984**, *106*, 2554. (b) Ziegler, T. *Organometallics* **1985**, *4*, 675.
(28) Stevens, A. E.; Beauchamp, J. L. *J. Am. Chem. Soc.*, in press. Referred to in ref 1.
(29) Goodman, J. L.; Peters, K. S.; Vaida, V. *Organometallics* **1986**, *5*, 815 and references therein.

trend-setting term in eq 14. We find in fact, in agreement with experiment,[26a] that $PA[Mn(CO)_5^-] > PA[Co(CO)_4^-]$, and we note that this order for the proton affinities is caused by $Co(CO)_4$ having a larger electron affinity than $Mn(CO)_5$ (Table VI). The proton affinities of $Tc(CO)_5^-$ and $Re(CO)_5^-$ are likewise seen to be larger than the proton affinities for $Rh(CO)_4^-$ and $Ir(CO)_4^-$, respectively, as a result of $Rh(CO)_4$ and $Ir(CO)_4$ having larger electron affinities than $Tc(CO)_5$ and $Re(CO)_5$, respectively. The increase in electron affinity as we move within the same transition series from $M(CO)_5$ with a metal center from the middle of the series to $M(CO)_4$ with a metal center from the end of the series correlates with a general decrease in the energy of *n*d toward the end of the three transition series. We expect within a given transition series $ML_n^-$ of the early or middle elements to have a larger proton affinity than $ML_n^-$ made up of the late elements for the "same" set of ligands.

The electron affinities of $M(CO)_5$ (M = Mn, Tc, Re) were calculated as the energy difference between $M(CO)_5^-$ of bipyramidal geometry and $M(CO)_5$ with the geometry of the $M(CO)_5$ framework in **12**. The electron affinities of $M(CO)_4$ (M = Co, Rh, Ir) were calculated as the energy difference between $M(CO)_4^-$ with a tetrahedral geometry and $M(CO)_4$ with the same geometry as the $M(CO)_4$ framework in **13**.

We have not studied in any great detail how other coligands than CO might modify $D(H-ML_n)$ and $PA[ML_n^-]$. However, substituting the carbonyl trans to the hydride in $HCo(CO)_4$ by the better $\sigma$-donor and poorer $\pi$-acceptor $PH_3$ to produce $HCo(CO)_3(PH_3)$ does only reduce the homolytic M-H bond strength by 11 kJ mol$^{-1}$, whereas $PA[Co(CO)_3PH_3^-]$ is seen to be 58 kJ mol$^{-1}$ smaller than $PA[Co(CO)_4^-]$ (Table VI). The reduction in the proton affinity caused by the phosphine substitution stems from $Co(CO)_3PH_3$ having a lower electron affinity than $Co(CO)_4$ (Table VI), as a result of the electron accepting metal (s,p,d)-hybride being more antibonding in $Co(CO)_3PH_3$ than in $Co(CO)_4$.[27b]

Our calculated value for $PA[Mn(Co)_5^-]$ of 1253 kJ mol$^{-1}$ compared reasonably well with $PA[Mn(CO)_5^-]$ = 1330 kJ mol$^{-1}$ obtained experimentally by Stevens and Beauchamp.[28] We have in a previous study[27b] calculated the proton affinity of $M(CO)_5^-$ (M = Mn, Tc, Re) and $M(CO)_4^-$ (M = Co, Rh, Ir) using the HFS method. The trends in the PAs are the same in the two studies, although the PAs calculated by the present method are some 35 kJ mol$^{-1}$ higher than the PAs evaluated by the HFS method.

## VIII. Concluding Remarks

We have studied the homolytic M-H and $M-CH_3$ bond energies in $MX^{n+}$ and $XM(CO)_m^{n+}$ of middle to late transition metals. We have found for the neutral molecules with $n = 0$ that the $M-CH_3$ bond is weaker than the M-H bond, in spite of the fact that $M-CH_3$ is stabilized relative to M-H by a stronger $\sigma$-bonding interaction as well as charge transfer from the occupied $\pi_{CH_3}$ orbitals to empty $nd_\pi$ or $(n+1)p_\pi$ metal orbitals, as a result of destabilizing exchange repulsions between the fully occupied $1\sigma_{CH_3}$ orbital and occupied metal orbitals. For the positively charged molecules with $n = 1$ the charge transfer from $CH_3$ to the metal center is enhanced and the exchange repulsions are reduced due to a contraction of the metal orbitals in the presence of the positive charge. The strength of the $M-CH_3$ bond is as a result increased to the point where the $M-CH_3$ bond becomes stronger than or as strong as the corresponding M-H bond. We have finally given an analysis of the factors responsible for periodic trends in the proton affinities $PA[M(CO)_m^-]$ of $M(CO)_m^-$. It is shown that the homolytic bond energies $D(H-M(CO)_m)$ of $HM(CO)_m$ as well as the electron affinities $A[M(CO)_m]$ of $M(CO)_m$ are responsible for the trends (increase) in $PA[M(CO)_m^-]$ down a triad, whereas $A[M(CO)_m]$ is responsible for the trends (decrease) along a period.

The calculations presented here are based on a relatively new[9] but well tested[9,14c] density functional method. We expect the bond energies obtained here to be accurate to within 50 kJ mol$^{-1}$ or less, with an even smaller error margin for the difference $D(H-M) - D(CH_3-M)$. We do not expect the conclusions drawn here to be changed by calculations based on extensive configuration interaction methods or more accurate density functionals.

**Acknowledgment.** We thank Professor E. J. Baerends and the theoretical chemistry group at the Free University in Amsterdam for providing us with a copy of their HFS program. This investigation was supported by the Natural Sciences and Engineering Research Council of Canada (NSERC) as well as Alberta Research Council through a scholarship to V. T. All calculations were carried out at the Cyber-205 installation at the University of Calgary.

# Reinterpretation of Surface-Enhanced Resonance Raman Scattering of Flavoproteins on Silver Colloids

**Nam-Soo Lee,[†+] You-Zung Hsieh,[†] Michael D. Morris,*[†] and Lawrence M. Schopfer*[‡]**

*Contribution from the Departments of Chemistry and Biological Chemistry, University of Michigan, Ann Arbor, Michigan 48109.* *Received August 14, 1986*

**Abstract:** The surface-enhanced resonance Raman scattering of riboflavin binding protein, glucose oxidase, lactate oxidase, *p*-hydroxybenzoate hydroxylase, Old Yellow Enzyme, and flavodoxin (*M. Elsdenii*) on colloidal silver has been investigated. The signals are shown to arise from free flavin extracted from the proteins. No spectra of flavins incorporated in proteins are observed.

Application of surface-enhanced Raman scattering (SERS) to proteins and surface-enhanced resonance Raman scattering (SERRS) to chromophores imbedded in proteins is under extensive investigation.[1] The application to small molecules of biological interest is now well-established.[2] Silver electrodes and colloidal

[†] Department of Chemistry.
[‡] Department of Biological Chemistry.
[+] Present Address: Department of Chemistry, Syracuse University, Syracuse, New York 13244.

(1) (a) Smulevich, G.; Spiro, T. G. *J. Phys. Chem.* **1985**, *89*, 5168-5173. (b) Sanchez, L. A.; Spiro, T. G. *Ibid.* **1985**, *89*, 763-768. (c) Copeland, R. A.; Fodor, S. P. A.; Spiro, T. G. *J. Am. Chem. Soc.* **1984**, *106*, 3872-3874. (d) Lee, N. S.; Sheng, R. S.; Schopfer, L. M.; Morris, M. D. *Ibid.* **1986**, *108*, 6179-6183.

0002-7863/87/1509-1358$01.50/0 